

# A Rapid MPPT Algorithm Based on the Research of Solar Cell's Diode Factor and Reverse Saturation Current

Liu Li-qun

Department of Electrical Engineering,  
Shanghai Jiaotong University,  
Shanghai, 200240, China;

Department of electronic and information ,  
Taiyuan University of Science & Technology,  
Taiyuan 030024, Shanxi Province, China  
Email: llqd2004@163.com

Wang Zhi-xin

Department of Electrical Engineering,  
Shanghai Jiaotong University,  
Shanghai, 200240, China;

wangzxin@sjtu.edu.cn

*Abstract:* - An efficient Maximum Power Point Tracking (MPPT) algorithm is important to increase the output efficiency of a photovoltaic (PV) generate system. The conventional method have some problems in that it is impossible to quickly acquire the generation power at the maximum power (MP) point, i.e., the efficiency of electric power generation is very low, and the amount of electric power generated by solar cell is always changing with weather conditions. Normally, the different solar cells have different diode factor ( $n$ ) and reverse saturation current ( $I_0$ ). Theoretical and simulative results show that the approximately linear relationship exists between the optimal output current and the short-circuit current, and if the weather conditions are sameness, a piece of solar cell have same photocurrent under different diode factor  $n$  and reverse saturation current  $I_0$  conditions. A new combined perturb and observe (PO) method is described in order to acquire the actual diode factor and reverse saturation current. This paper describes a rapid maximum power point tracking method which is based on the actual  $n$  and  $I_0$ . An expiatory program is applied to acquire the actual maximum power point. The correctness and validity of expiatory coefficients is verified through simulation. The simulation results verified the correctness and validity of MPPT algorithm.

*Key-Words:* - Maximum Power Point Tracking (MPPT), Renewable energy, Photovoltaic (PV) system, Diode factor, Reverse saturation current, Photocurrent

## 1 Introduction

Renewable energy sources, such as solar, wind, biomass, etc., are desirable for electrical power generate due to their unlimited existence and environmental friendly nature [1]. PV technology has been developed rapidly over the last two decades from a small-scale, specialist industry supplying the U.S. space program to a broadly based global activity [2]. Studies on PV generate systems are actively being promoted in order to mitigate environmental issues such as the green house effect and air pollution [3-4]. In developing nations, the PV generate system is expected to play an important role in total electrical energy demand, and solar photovoltaic energy has gained a lot of attention because it is renewable, friendly to the environment, and flexible for installation. And more and more specialist of China realized the fundamentality of PV generate systems. A photovoltaic generate system consists of a number of solar cells depending

on the required power, voltage and current ratings, and the solar cell price is decreasing. But a photovoltaic generate system still requires expensive initial investments. In order to extract as much energy as possible from a PV system, it is important to have an efficient Maximum Power Point Tracking algorithm.

Many MPPT algorithms and control schemes of PV generate system have been proposed in the literature [1-10], i.e., a cost-effective single-stage control scheme is proposed in the literature[1], it proposes a cost-effective single-stage inverter with maximum power point tracking (MPPT) in combination with one-cycle control (OCC) for photovoltaic power generation. A comparative study of the maximum power point trackers using a switching-frequency modulation scheme (SFMS) for photovoltaic panels is presented [2]. Method of locating the maximum power point (MPP) is based on injecting a small-signal sinusoidal perturbation

into the switching frequency of the converter and comparing the ac component and the average value of the panel's terminal voltage. The linearity method is a novel method in order to track the maximum power point [3-4], the proportionality coefficient of the prediction line is automatically corrected using the hill-climbing method when the panel temperature of the solar arrays is changed. The incremental conductance (IC) method is proposed in the literature [5], which is based on the Incremental Conductance method but does not require any current sensing devices. The perturbation and observation (PO) method is well known as the hill-climbing method, it has been widely used because of its simple feedback structure and fewer measured parameters. A digital hill-climbing control strategy combined with a bidirectional current mode power cell is presented which allows getting a regulated bus voltage topology [6]. A simple method which combines a discrete time control and a PI compensator is proposed [7], the object of this paper is to investigate the maximum power tracking algorithms which were often used to compare the tracking efficiencies for the system operating under different controls. The constant voltage (CV) and perturbation and observation (PO) method are very common, a cost-effective two-method MPPT control scheme is proposed in this paper to track the maximum power point (MPP) at both low and high irradiation, by combining a Constant Voltage (CV) method and a modified PO algorithm [8]. The fuzzy methods are described in the literature [9-12] that focus on the nonlinear characteristics of solar cell. A power management system is presented [13], which allows for maximum exploitation of the solar energy. Although, various methods of MPPT control have been proposed in existing literature, but the power generate efficiency is relative low, and the amount of electric power generated by solar arrays is always changing with weather conditions. Different solar panel have different diode factor ( $n$ ) and reverse saturation current ( $I_0$ ). So they are impossible to quickly acquire the generate power at the maximum power point (MPP). The essential reason is the unknown values of  $n$  and  $I_0$ . The theoretical and simulative results show that not only the optimal output current and short-circuit current have an approximate linear relationship at a constant temperature. But also if the weather conditions are sameness, a piece of solar cell have same photocurrent under different diode factor  $n$  and reverse saturation current  $I_0$  conditions. The conclusion is very important to acquire the actual diode factor and reverse saturation current.

In this paper, first, theoretical and simulative results show that a piece of solar cell have same photocurrent under different diode factor  $n$  and reverse saturation current  $I_0$  conditions, and a novel combined perturb and observe (PO) method is described in order to acquire the actual  $n$  and  $I_0$ . Next, the approximately linear relationship exists between the optimal output current and the short-circuit current is described. Finally, an expiatory program is applied to acquire the actual maximum power point, and a rapid maximum power point tracking method is described which is based on the actual  $n$  and  $I_0$ . The simulative results verified the correctness and validity of MPPT algorithm.

## 2 Principle analyzing and modeling of solar cell

### 2.1 Solar cell modeling

Various modelling of solar cell have been proposed in the literature [3-10]. The output current  $I$  and output voltage  $V$  of solar cell is given by (1) and (2) using the symbols in Fig. 1, i.e.,

$$I = I_{ph} - I_d - V_d / R_{sh} \quad (1)$$

$$V = V_d - R_s I \quad (2)$$

$$I_d = I_0 \left[ \exp\left(\frac{qV_d}{nkT}\right) - 1 \right] \quad (3)$$

here  $I_{ph}$  is the photocurrent (in amperes),  $I_0$  is the reverse saturation current (in amperes),  $I_d$  is the average current through diode (in amperes),  $n$  is the diode factor,  $q$  is the electron charge (in coulombs),  $q = 1.6 \times 10^{-19} C$ ,  $k$  is Boltzmann's constant (in joules per Kelvin),  $k = 1.38 \times 10^{-23} J / K$ , and  $T$  is the solar arrays panel temperature (in Kelvin).  $R_s$  is the intrinsic series resistance of the solar cell. Normally, the value of  $R_s$  is very small (in milliohm).  $R_{sh}$  is the equivalent shunt resistance of the solar array, and the value is very large (in kilo-ohm). In general, the output current of solar cell is expressed by

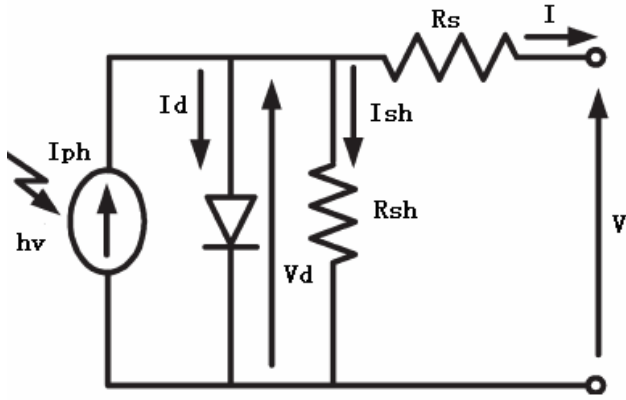


Fig.1, Equivalent circuit for solar cell

$$I = I_{ph} - I_o \left[ \exp\left\{ \frac{q}{nkT} (V + R_s I) \right\} - 1 \right] - \frac{V + R_s I}{R_{sh}} \quad (4)$$

Where the resistances  $R_s$  and  $R_{sh}$  can generally be neglected, and (4) is simplified to (5).

$$I = I_{ph} - I_o \left[ \exp\left\{ \frac{q}{nkT} (V) \right\} - 1 \right] \quad (5)$$

If the circuit is opened, the output current  $I = 0$ , and the open-circuit voltage  $V_{oc}$  is expressed by

$$V_{oc} = V_{max} = \frac{nkT}{q} \ln\left(\frac{I_{ph}}{I_o} + 1\right) \approx \frac{nkT}{q} \ln\left(\frac{I_{ph}}{I_o}\right) \quad (6)$$

If the circuit is shorted, the output voltage  $V = 0$ , the average current through diode  $I_d$  is generally be neglected, and the short-circuit current  $I_{sc} = I$  is expressed by using (7). The relationship exists between short-circuit current  $I_{sc}$  and photocurrent  $I_{ph}$  by using (8).

$$I = I_{ph} - \frac{R_s I}{R_{sh}} \quad (7)$$

$$I = I_{sc} = I_{ph} / \left(1 + \frac{R_s}{R_{sh}}\right) \approx I_{ph} \quad (8)$$

Finally, the output power  $P$  is expressed by (9)

$$P = IV = (I_{ph} - I_d - V_d / R_{sh})V = (I_{ph} - I_d)V = (I_{ph} - I_o \left[ \exp\left[ \frac{q}{nkT} (V) \right] - 1 \right])V \quad (9)$$

$$P_{max} = I_{ph} V_{oc} - \frac{nkT}{q} \ln\left(1 + \frac{qV_{mppt}}{nkT}\right) - \frac{V_{oc}}{qV_{mppt}(nkT)} + \left(\frac{nkT}{q}\right)^2 \frac{1}{V_{mppt}} \ln\left(1 + \frac{qV_{mppt}}{nkT}\right) \quad (10)$$

Here  $P$  and  $V$  are the instantaneous output power and output voltage of solar cell, respectively. The condition of the maximum power point is  $\partial P / \partial V = 0$ . The maximum power  $P_{max}$  is expressed by (10). Here  $P_{max}$  and  $V_{mppt}$  are the maximum output power and optimal output voltage at the time, respectively.

$$I_{sc} = I_{sc}(25^\circ C, 1KW/m^2) \times S / 1000 \quad (11)$$

$$I_{ph}(25^\circ C, 1KW/m^2) = I_{sc}(25^\circ C, 1KW/m^2) \times (1 + R_s / R_{sh}) \approx I_{sc}(25^\circ C, 1KW/m^2) \quad (12)$$

$$I_{ph} = I_{ph}(25^\circ C, 1KW/m^2) \times [1 + K_i \times (T - T_r)] \times (1 + R_s / R_{sh}) \times S_j / 1000 \quad (13)$$

$$S = \frac{I_{ph} \times 1000}{I_{ph}(25^\circ C, 1KW/m^2) \times [1 + K_i \times (T - T_r)] \times (1 + R_s / R_{sh})} \quad (14)$$

$$I_{m\ popt} = I_{ph} \left[ 1 - \exp\left(\frac{V_{mppt} - V_{oc}}{nkT}\right) \right] \quad (15)$$

Various parameters affect the output power, i.e., two intrinsic resistances, the temperature, the irradiation, the diode factor and the reverse saturation current. Firstly,  $R_s$  is very small (mΩ), and  $R_{sh}$  is very large (in kilo-ohm). The effect of two intrinsic resistances is ignored under ideal condition. The values of two intrinsic resistances are the unknown constants. Secondly, the important factors are temperature and irradiation. The short-circuit current  $I_{sc}$  and the open-circuit voltage  $V_{oc}$  of solar cell are always changing with the temperature and irradiation. If the temperature is changeable, the changing coefficient  $K_v$  of  $V_{oc}$  is  $(-0.37 - -0.4\%) / ^\circ C$  at solar panel temperature  $25^\circ C$ , the changing coefficient  $K_i$  of  $I_{sc}$  is  $(+0.09 - +0.1\%) / ^\circ C$  at solar panel temperature  $25^\circ C$ , where,  $T_r$  are  $25^\circ C$  (in Kelvin). If the irradiation is changeable, the short-circuit current  $I_{sc}$  is expressed by using (11) at temperature  $25^\circ C$ . Here  $I_{sc}(25^\circ C, 1KW/m^2)$  is the short-circuit current at solar panel temperature  $25^\circ C$ , and the irradiation is  $1KW/m^2$ . The relationship exists between short-circuit current  $I_{sc}(25^\circ C, 1KW/m^2)$  and photocurrent  $I_{ph}(25^\circ C, 1KW/m^2)$  is expressed by using (12) at solar panel temperature  $25^\circ C$ , and the irradiation is  $1KW/m^2$ . The photocurrent  $I_{ph}$  is expressed by using (13) with the temperature and irradiation changing. Thus, using (6) and (13), the open-circuit voltage  $V_{oc}$  is evaluation. Thirdly, the diode factor  $n$  and reverse saturation current  $I_o$  affect the output power. The  $n$  and  $I_o$  are the unknown constant. Although different solar cells have different  $n$  and  $I_o$ , a piece of solar cell's  $n$  and  $I_o$  is same. Normally, the  $n$  exists between 40 and 110, and the  $I_o$  exists between  $0.2 \mu A$  and  $500 \mu A$ . If the value of  $n$  and  $I_o$  are known, the method is easy to acquire a piece of solar cell's maximum output power. The effect of  $n$  and  $I_o$  are analysed in this paper. The irradiation  $S$  is expressed (14) as a function of  $I_{ph}$ . The optimal output current is given by (15) as a function of the optimal output voltage  $V_{mppt}$  using circuit parameters  $q$ ,  $n$ ,  $k$ ,  $T$ .

## 2.2 Relationship of n, I<sub>o</sub> and I<sub>ph</sub>

For example, the open-circuit voltage  $V_{oc}$  and short-circuit current  $I_{sc}$ , which were measured at irradiation  $1KW/m^2$  and temperature  $25^{\circ}C$ , are  $22V$  and  $3.8A$ , respectively. The changing coefficient  $K_i$  of  $I_{sc}$  and the changing coefficient  $K_v$  of  $V_{oc}$  were measured, are  $0.001$  and  $-0.004$ , respectively. Fig. 2 shows P-I characteristics and  $P_{max}$  curve of solar cell, the data are calculated by using above values under the same  $n$  and different  $I_0$  conditions. Fig.2 (a) shows the maximum power curve at same irradiation and different temperature, Fig.2 (b) shows the maximum power curve at same temperature and different irradiation.

If the irradiation is  $800W/m^2$ , and the temperature is changing from  $-50^{\circ}C$  to  $75^{\circ}C$ , under same diode factor  $n$  and different reverse saturation current  $I_0$  conditions, Fig. 2 (a) shows that the photocurrent  $I_{ph}$  is same under same temperature conditions, and the output power is increasing with the  $I_0$  decreasing from  $500\mu A$  to  $0.2\mu A$ . If the temperature is  $25^{\circ}C$ , and the irradiation is changing from  $100W/m^2$  to  $1KW/m^2$ , under same diode factor  $n$  and different reverse saturation current  $I_0$  conditions, Fig. 2 (b) shows that the photocurrent  $I_{ph}$  is same under same irradiation conditions, and the output power is increasing with the  $I_0$  decreasing from  $500\mu A$  to  $0.2\mu A$ .

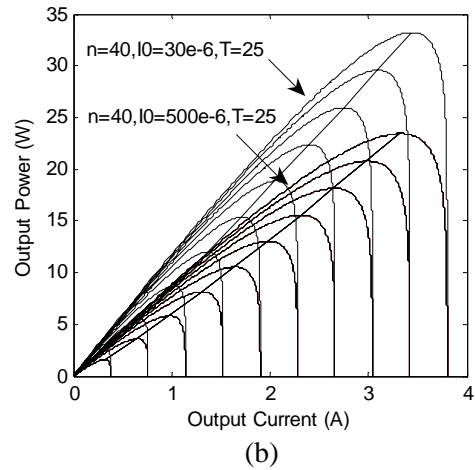
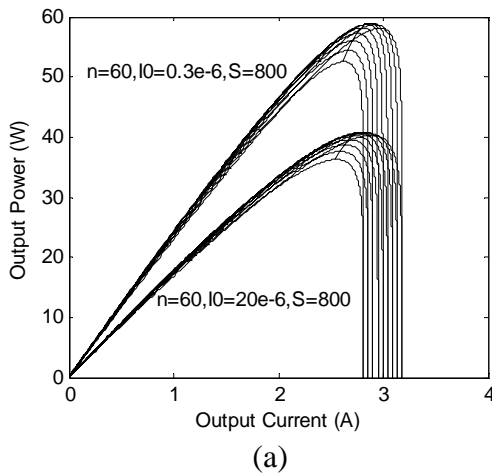
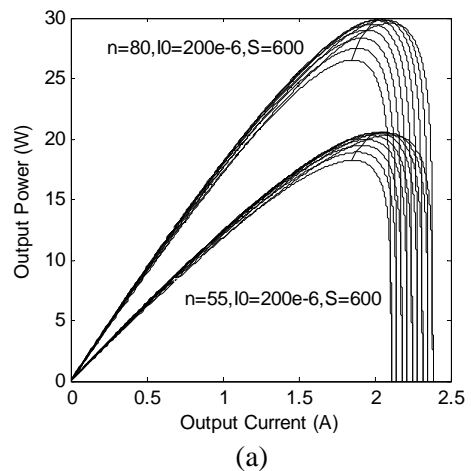


Fig.2 Calculated P-I characteristics and  $P_{max}$  curve under the same  $n$  and different  $I_0$  conditions. (a) The irradiation  $S$  is  $800W/m^2$ , and the temperature is changing from  $-50^{\circ}C$  to  $75^{\circ}C$ . (b) The irradiation is changing from  $100W/m^2$  to  $1KW/m^2$  at the temperature  $25^{\circ}C$ .

If the irradiation is  $600W/m^2$ , and the solar panel temperature is changing from  $-50^{\circ}C$  to  $75^{\circ}C$ , under same  $I_0$  and different  $n$  conditions, Fig.3 (a) shows that the photocurrent  $I_{ph}$  is same under same temperature conditions and the output power is increasing with the  $n$  increasing from  $40$  to  $110$ . If the irradiation is changing from  $100W/m^2$  to  $1KW/m^2$  at the temperature  $35^{\circ}C$ , Fig.3 (b) shows that the photocurrent  $I_{ph}$  is same at same irradiation, and the output power is increasing with the  $n$  increasing from  $40$  to  $110$ .



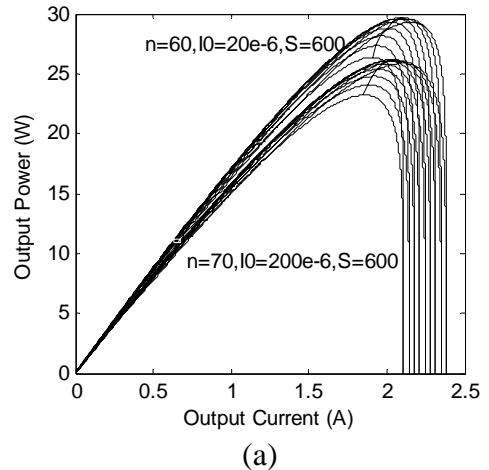
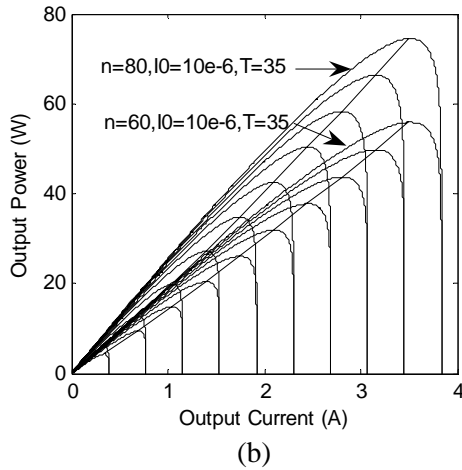


Fig.3 Calculated P-I characteristics and  $P_{max}$  curve under the different  $n$  and same  $I_0$  conditions. (a) The irradiation  $S$  is  $600W/m^2$ , and the temperature is changing from  $-50^{\circ}C$  to  $75^{\circ}C$ . (b) The irradiation is changing from  $100W/m^2$  to  $1KW/m^2$  at temperature  $35^{\circ}C$ .

If the weather conditions are same, Fig. 4 shows that the output photocurrent  $I_{ph}$  is same under different diode factor  $n$  and different reverse saturation current  $I_0$  conditions. If the irradiation is  $600W/m^2$ , and the temperature is increasing from  $-50^{\circ}C$  to  $75^{\circ}C$ , Fig. 4 (a) shows that the photocurrent  $I_{ph}$  is same under different diode factor  $n$  and different reverse saturation current  $I_0$  conditions. If the temperature is  $45^{\circ}C$ , and the irradiation is increasing from  $100W/m^2$  to  $1KW/m^2$ , Fig.4 (b) shows that the photocurrent  $I_{ph}$  is same under different diode factor  $n$  and different reverse saturation current  $I_0$  conditions.

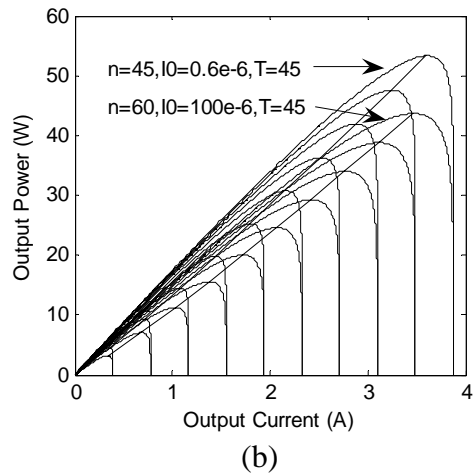


Fig.4 Calculated P-I characteristics and  $P_{max}$  curve under different  $n$  and  $I_0$ . (a) If the irradiation  $S$  is  $600W/m^2$ , and the temperature is changing from  $-50^{\circ}C$  to  $75^{\circ}C$ . (b) If the irradiation is changing from  $100W/m^2$  to  $1KW/m^2$  at temperature  $45^{\circ}C$ .

A conclusion is gained in this paper. If the weather conditions are same, a piece of solar cell's output photocurrent  $I_{ph}$  is same under different diode factor  $n$  and different reverse saturation current  $I_0$  conditions. The conclusion is very important to acquire the maximum power point of PV system. Based on the conclusion, a novel method was presented to acquire the actual diode factor and reverse saturation current.

### 2.3 Acquire the actual $n$ and $I_0$

In this case, firstly, the diode factor  $n$  and reverse saturation current  $I_0$  were supposed, are 40 and  $500\mu A$ , respectively. The output voltage  $V$ , the output current  $I$  and temperature  $T$  of the solar panel, which were detected by using sensors, are the voltage sensor, current sensor and temperature sensor, respectively. The photocurrent  $I_{ph}$  is given by using (5), and the assumptive maximum power point was acquired. Fig.5 shows the assumptive maximum power point A of solar cell by using the assumptive  $n$  and  $I_0$  under steady weather conditions. Secondly, Fig.5 shows the actual maximum power point B by using Perturb and Observe method under same weather conditions. The actual optimal output current  $I_{mppt}$  and optimal output voltage  $V_{mppt}$  is gained by using sensors. As shown in Fig.5, the photocurrent  $I_{ph}$  is

same under same weather conditions. Finally, the diode factor  $n$  is supposed minimum and the reverse saturation current  $I_0$  is supposed maximum. The actual maximum power is more than the assumptive maximum power. Based on above conclusion, the diode factor  $n$  should increase and the reverse saturation current  $I_0$  should decrease in order to acquire the actual  $n$  and  $I_0$ . Based on the increasing diode factor  $n$  and the decreasing reverse saturation current  $I_0$ , the photocurrent  $I_{ph}$  and actual optimal output voltage  $V_{mppt}$  is used to calculate the assumptive optimal output current  $I_{mppt1}$  by using (5). Then, the difference between the actual optimal output current and assumptive optimal output current is  $\Delta I (= I_{mppt1} - I_{mppt})$ . If the  $\Delta I = 0$ , the diode factor  $n$  and reverse saturation current  $I_0$  are actual value. Thus, the actual value of  $n$  and  $I_0$  was saved, and PO method is stopped.

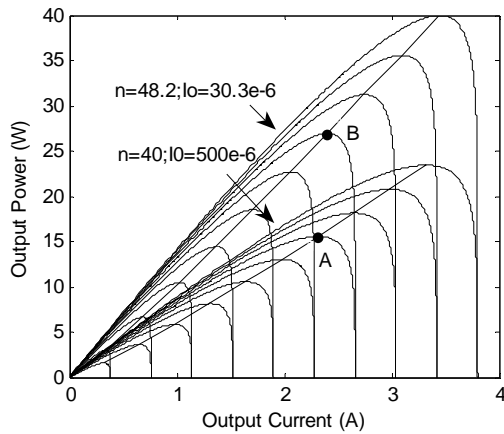


Fig.5 Calculated the actual diode factor  $n$  and reverse saturation current  $I_0$  by using the combined perturb and observe (PO) method.

Next, the process cited above is concretely explained by examples with number obtained based on Fig.5. First, the output voltage and output current were measured at time  $n_1$ , are  $7.0573V$  and  $2.1812A$ , respectively. In this case, the generated power  $P(n_1)$  is  $15.3934W$ . The temperature  $T$  of solar panel is  $25^\circ C$  at time  $n_1$ . Then, the diode factor  $n$  and reverse saturation current  $I_0$  were supposed, are  $40$  and  $500\mu A$ , respectively. The photocurrent  $I_{ph} = 2.66A$  is gained by using (5). The irradiation  $S$  is  $700W/m^2$  by using (14). The temperature and irradiation are steady at enough long time. The calculated optimal output current and optimal output voltage were gained, are  $2.3089A$  and  $6.7400V$ , respectively. The calculated optimal output power  $P_{max}'(n_1)$  is  $15.562W > P(n_1)$ . Second, the PO method is utilized to acquire the actual maximum power point under

same weather conditions. The actual optimal output current  $I_{mppt}(n_1)$  and optimal output voltage  $V_{mppt}(n_1)$  were measured, are  $2.396A$  and  $11.24V$ , respectively. Thus, the maximum output power  $P_{max}(n_1)$  is  $26.9310W$ , and  $(P_{max}(n_1) > P_{max}'(n_1))$ . Based on above conclusion, in order to acquire the actual  $n$  and  $I_0$  of a piece of solar cell it is obligatory to increase the diode factor  $n$  and decrease the reverse saturation current  $I_0$ . In this case, the actual optimal output voltage  $V_{mppt}(n_1)$  and photocurrent  $I_{ph}$  were used to calculate the assumptive optimal output current  $I_{mppt1}$  by using (5). Then, the difference  $\Delta I$  between the actual optimal output current and assumptive optimal output current is calculated. If  $\Delta I = 0$ , the actual value of the diode factor  $n$  and reverse saturation current  $I_0$  is gained, are  $48.2$  and  $30.3e-6$ , respectively. The values of actual  $n$  and  $I_0$  were saved.

### 3 The proposed MPPT algorithms

For instance, in the case of solar cell,  $V_{oc}$ ,  $I_{sc}$ ,  $R_s$ ,  $R_{sh}$ ,  $K_i$ ,  $K_v$ ,  $n$ , and  $I_0$  at irradiation  $1K/m^2$  and temperature  $25^\circ C$ , are  $22V$ ,  $3.8A$ ,  $8m\Omega$ ,  $10K\Omega$ ,  $0.001$ ,  $-0.004$ ,  $60$  and  $10 \times 10^{-6}A$ , respectively. Fig. 6 shows  $V-I$  characteristics and  $P_{max}$  curve of solar cell are calculated using above values. Fig.6 (a) shows the maximum power curve at different temperature and same irradiation  $600W/m^2$ , Fig.6 (b) shows the maximum power curve at same temperature  $25^\circ C$  and different irradiation. It is confirmed through calculating results shown in Fig. 6 that a proportional relationship between the short-circuit current and the optimal output current have been proposed in the literature [3], [4]. The proportionality coefficient using  $K_x$ ,  $K_x$  is  $I_{mppt}(n)/I_{sc}(n)$ , which is the coefficient of the optimum output current and the short-circuit current at the time. Normally, it exists between  $0.9$  and  $0.95$ . The simulative and calculated results verified that an error exists between the maximum power curve and the power curve at  $K_x = 0.9 \sim 0.95$ . Based on the simulative conclusion, if the irradiation  $S$  is more than  $150W/m^2$ , the coefficient  $K_x$  exists between  $0.87$  and  $0.95$  under different  $n$  and different  $I_0$ . The irradiation  $S$  is less than  $150W/m^2$ , the coefficient bound is different. Normally, it exists between  $0.8$  and  $0.87$  under different  $n$  and different  $I_0$ .

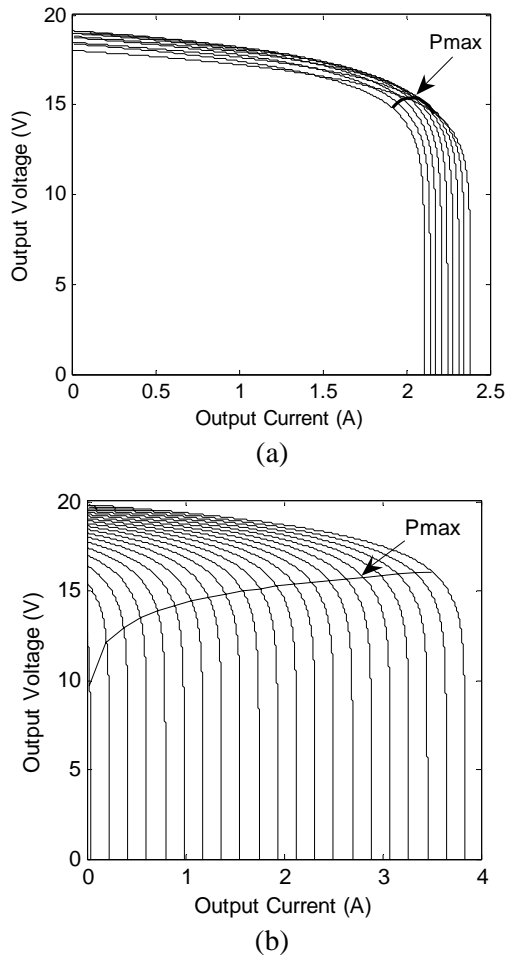


Fig.6 Calculated V-I characteristics and  $P_{max}$  curve. (a) If the irradiation is  $600W/m^2$ , and the temperature is changed from  $-25^{\circ}C$  to  $75^{\circ}C$ . (b) If the irradiation is changed from  $50W/m^2$  to  $1KW/m^2$  at temperature  $25^{\circ}C$ .

For instance, the diode factor  $n$  and the reverse saturation current  $I_0$  were supposed, are 40 and  $500\mu A$ , respectively. Other factors are same. Fig. 7 (a) shows the P-I characteristics, and draws a comparison between the  $P_{max}$  curve and the  $P_{max}'$  curve at  $K_x=0.9$  and  $K_x=0.95$  under same irradiation  $1KW/m^2$  and various temperatures. Fig. 7 (b) shows the P-I characteristics, and draws a comparison between the  $P_{max}$  curve and the  $P_{max}'$  curve at  $K_x=0.9$  and  $K_x=0.95$  under same temperature  $25^{\circ}C$  and various irradiation conditions. As shown in Fig. 7, the bound of coefficient  $K_x$  is not very accurate in the literature [3], [4].

Base on above conclusion, a proposed MPPT algorithm is described. If the diode factor  $n$  and the reverse saturation current  $I_0$  are known quantities by using the combined perturb and observe (PO) method. The effect of the temperature, the irradiation, the diode factor and the reverse

saturation current must be considered in order to acquire the maximum power point.

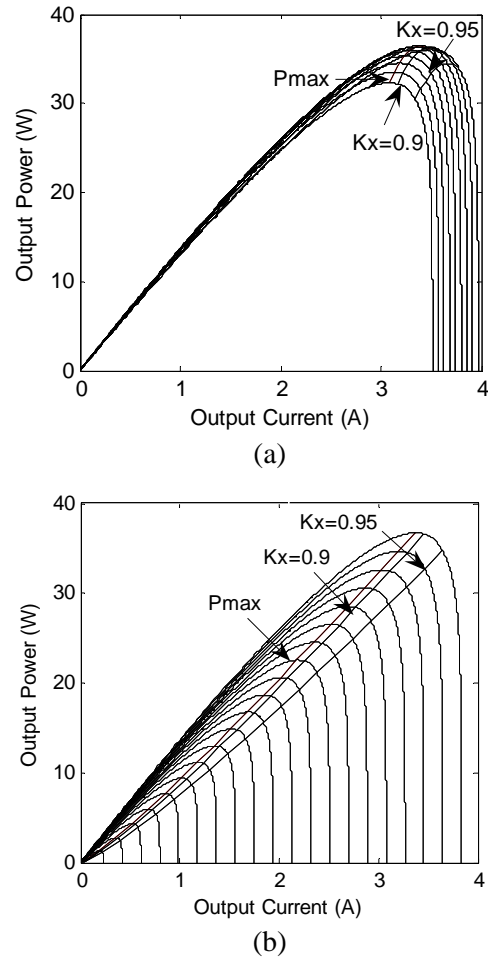


Fig.7 Draw a comparison between  $P_{max}$  curve and  $P_{max}'$  curve at  $K_x=0.9$  and  $K_x=0.95$ . (a) If the irradiation is  $1000W/m^2$ , the temperature is changing from  $-50^{\circ}C$  to  $75^{\circ}C$ . (b) If the irradiation is changing from  $50W/m^2$  to  $1KW/m^2$  at temperature  $25^{\circ}C$ .

The diode factor  $n$ , the reverse saturation current  $I_0$  and the coefficient  $K_x$  were supposed, are 60,  $0.25\mu A$  and 0.87, respectively. The  $P_{max}$  curve, P-I characteristic, and calculating  $P_{max}'$  curve at irradiation  $800W/m^2$  and different temperature show in Fig. 8 (a). The error between  $P_{max}$  and  $P_{max}'$  is big as Fig.8 (a) shows. Fig. 8 (b) shows that P-I characteristics,  $P_{max}$  curve and the calculatingly  $P_{max}'$  curve at the temperature  $25^{\circ}C$  and different irradiation. The error between  $P_{max}$  and  $P_{max}'$  is big as Fig.8 (b) shows. Theoretical and simulation results show that the effect of temperature and irradiation must be considered. The reverse saturation current  $I_0$  has an important effect in order to acquire the actual  $K_x$ . The effect of diode factor  $n$  is very small. In order to

acquire the actual  $K_x$ , the expiations of the temperature, irradiation and reverse saturation current  $I_0$  are necessary.

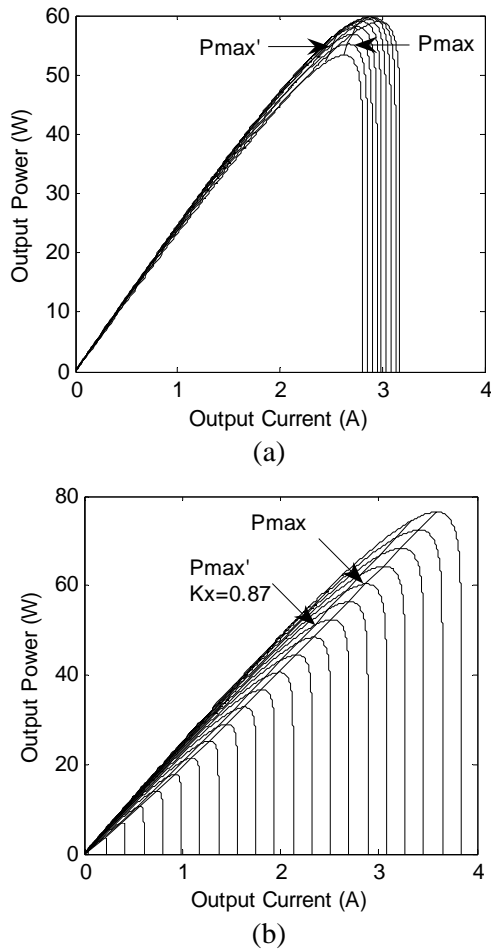
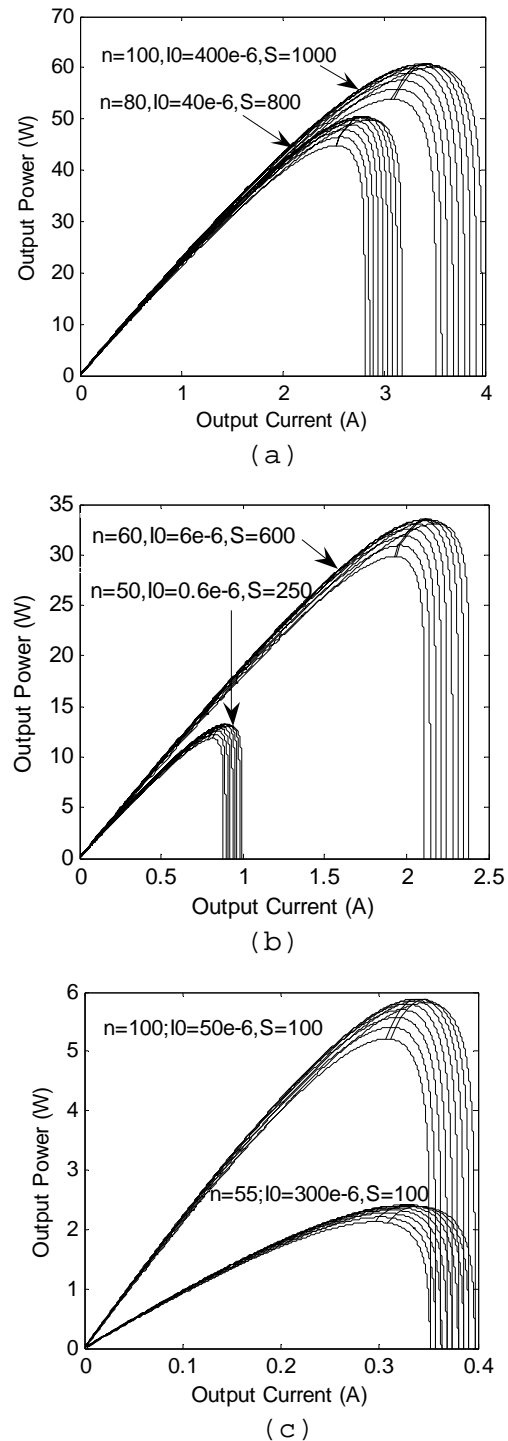


Fig.8 Draw a comparison between  $P_{max}$  curve and  $P_{max}'$  curve. (a) Under same irradiation conditions, the temperature is changing from  $25^{\circ}C$  to  $75^{\circ}C$ . (b) Under same temperature conditions, the irradiation changing from  $50 W / m^2$  to  $1KW / m^2$ .

Using (14), the irradiation can be gained at time  $m$ . Theoretical and simulation results show that the expiatory coefficient  $\Delta K_s$  of irradiation is expressed (16) as a function of the irradiation  $S$ . The expiatory coefficient is 0.3 when the irradiation  $S$  is less than  $100 W / m^2$ . The expiatory coefficient is  $-0.00073 m^2 / W$  from 0.1 with the irradiation increasing from  $100 W / m^2$  to  $200 W / m^2$ . The expiatory coefficient is  $-0.00009 m^2 / W$  from 0.041 with the irradiation increasing from  $200 W / m^2$  to  $400 W / m^2$ . The expiatory coefficient is  $-0.00004 m^2 / W$  from 0.023 with the irradiation increasing from  $400 W / m^2$  to  $700 W / m^2$ . Or else, the expiatory coefficient is  $0.00002 m^2 / W$  from 0.0176 with the irradiation increasing.

Theoretical and simulation results show that the expiatory coefficient  $\Delta K_t$  of temperature is

expressed (17) as a function of the temperature  $T$ . The expiatory coefficient is a constant from temperature  $-50^{\circ}C$  to  $-25^{\circ}C$ . The expiatory coefficient is  $-0.00004 / ^{\circ}C$  from 0.001 with the temperature increasing from  $-25^{\circ}C$  to  $5^{\circ}C$ . The expiatory coefficient is zero from temperature  $5^{\circ}C$  to  $35^{\circ}C$ . Or else, the expiatory coefficient is  $-0.00002 / ^{\circ}C$ . Here,  $T_{r1}$  is the actual solar panel temperature.



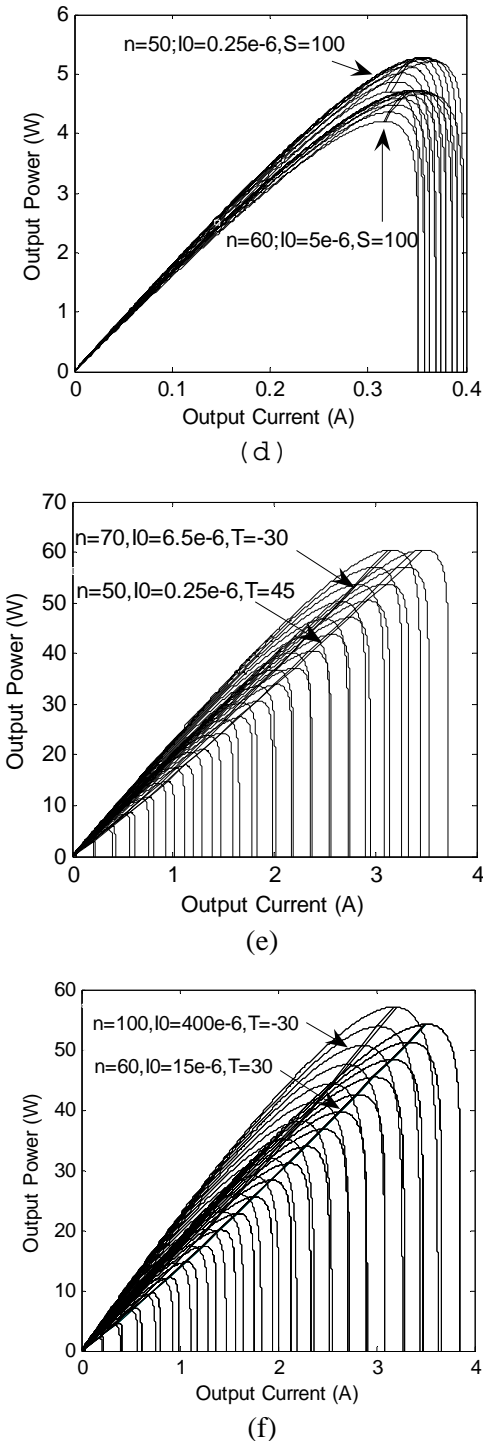


Fig.9 The  $P_{max}$  curve and  $P_{max}'$  curve are simulated under different  $n$  and different  $I_o$  conditions. (a)The  $I_o$  is more than  $10 \mu A$ . (b) The  $I_o$  is less than  $10 \mu A$ . (c) The  $I_o$  is more than  $10 \mu A$ , and the  $S$  less than  $150 W/m^2$ . (d) The  $I_o$  is less than  $10 \mu A$ , and the  $S$  less than  $150 W/m^2$ . (e) The  $I_o$  less than  $10 \mu A$ , and the  $n$  and  $T$  are different. (f) The  $I_o$  more than  $10 \mu A$ , and the  $n$  and  $T$  are different.

The expiation coefficient  $\Delta KI_o$  of reverse saturation current  $I_o$  is expressed (18) as a function

of  $I_o$ . The expiation coefficient is  $5.35e-5/\mu A$  from 0.005 with the reverse saturation current  $I_o$  increasing when the value of  $I_o$  is more than  $10\mu A$ . Or else, the expiation coefficient is  $5.35e-5/\mu A$  from 0.02 with the reverse saturation current  $I_o$  increasing.

$$\Delta Ks = \begin{cases} 0.1 & S \leq 100 W/m^2 \\ 0.1 - 0.0007 \times S & S \leq 200 W/m^2 \\ 0.041 - 0.00009 \times (S - 200) & S \leq 400 W/m^2 \\ 0.023 - 0.00004 \times (S - 400) & S \leq 700 W/m^2 \\ 0.0176 - 0.00002 \times (S - 700) & S > 700 W/m^2 \end{cases} \quad (16)$$

$$\Delta Kt = \begin{cases} 0.001 & Tr \leq -25^\circ C \\ 0.001 - 0.00004 \times (Tr + 25) & Tr \leq 5^\circ C \\ 0 & Tr \leq 35^\circ C \\ -0.00002 \times (Tr - 35) & Tr \leq 75^\circ C \end{cases} \quad (17)$$

$$\Delta KI_o = \begin{cases} 0.005 + (5.35e-5) \times \frac{(5e-4) - I_o}{(5e-4)} \times 500 & I_o \geq 10e-6 \\ 0.02 + (5.35e-5) \times \frac{(5e-4) - I_o}{(5e-4)} \times 500 & I_o < 10e-6 \end{cases} \quad (18)$$

$$Kxp = 0.87 - \Delta Ks + \Delta Kt + \Delta KI_o \quad (19)$$

The integrated expiation coefficient  $Kxp$  is expressed (19). Fig.9 shows the simulation results under different  $n$  and different  $I_o$  conditions. As shown in Fig.9 (a), the expiation coefficient is reasonable under the  $I_o$  is more than  $10 \mu A$  conditions. Fig.9 (b) shows that the expiation coefficient is reasonable under the  $I_o$  is less than  $10 \mu A$  conditions. As shown in Fig.9 (c), the expiation coefficient is reasonable under the  $I_o$  is more than  $10 \mu A$  conditions at low irradiation. As shown in Fig.9 (d), the expiation coefficient is reasonable under the  $I_o$  is less than  $10 \mu A$  conditions at low irradiation. Fig.9 (e) shows that the expiation coefficient is reasonable under the  $I_o$  is less than  $10 \mu A$  and different  $n$  and different  $T$  conditions. Fig.9 (f) shows that the expiation coefficient is reasonable under the  $I_o$  is more than  $10 \mu A$  and different  $n$  and different  $T$  conditions.

Based on the results of Fig. 9, no matter how the solar radiation and solar panel temperature change, the maximum power point is gained by using the integrated expiation coefficient  $Kxp$ . The maximum power point is gained by using the integrated expiation coefficient  $Kxp$  no matter how the values of the diode factor  $n$  and the reverse saturation current  $I_o$  vary with various solar cell. Based on the simulative results, the output efficiency of proposed MPPT algorithm is more than 99% under different  $n$  and different  $I_o$  and most weather conditions.

For instance, in the case of solar cell, the diode factor  $n$ , the reverse saturation current  $I_o$ , and the temperature  $T$ , are  $50, 0.6\mu A$ , and  $75^\circ C$ , respectively. The proportionality coefficient using  $KI$ ,  $KI$  is  $Imppt'/Imppt$ . It is the coefficient of the calculated optimum output current and the actual optimum output current. The proportionality coefficient using  $KV$ ,  $KV$  is  $Vmppt'/Vmppt$ . It is the coefficient of the calculated optimum output voltage and the actual optimum output voltage under various irradiation conditions. The proportionality coefficient using  $KP$ ,  $KP$  is  $Pmppt'/Pmppt$ . It is the coefficient of the calculated maximum output power and the actual maximum output power under different irradiation conditions. As shown in Table 1, if the irradiation is more than  $100W/m^2$ , the output efficiency of proposed MPPT algorithm is more than 99% under different  $n$  and different  $I_o$  and various weather conditions.

Table 1 Simulative results of high irradiation.

S	KI	KV	KP
$100W/m^2$	0.9928	1.0091	0.9994
$200W/m^2$	0.9730	1.0242	0.9957
$300W/m^2$	0.9807	1.0178	0.9976
$400W/m^2$	0.9887	1.0109	0.9991
$500W/m^2$	0.9917	1.0080	0.9995
$600W/m^2$	0.9948	1.0053	0.9998
$700W/m^2$	0.9914	1.0084	0.9995
$800W/m^2$	0.9931	1.0067	0.9996
$900W/m^2$	0.9946	1.0051	0.9998
$1000W/m^2$	0.9964	1.0036	0.9999

For instance, the diode factor  $n$ , the reverse saturation current  $I_o$ , and the temperature  $T$ , are  $60, 7.3\mu A$ , and  $35^\circ C$ , respectively. The irradiation is less than  $100W/m^2$ . As shown in Table 2, the output efficiency of solar cell is more than 98%. A conclusion is gained in this paper. Not matter the irradiation and the temperature are varying with the weather, the proposed MPPT algorithm is high efficiency to track the maximum output power of solar cell, and large numbers of calculation is not essential.

Table 2 Simulative results of low irradiation.

S	Pmppt'	Pmppt	KP
$10W/m^2$	0.3280W	0.3336W	0.9833
$20W/m^2$	0.7267W	0.7381W	0.9846
$30W/m^2$	1.1510W	1.1700W	0.9837
$40W/m^2$	1.5928W	1.6198W	0.9834
$50W/m^2$	2.0459W	2.0828W	0.9822
$60W/m^2$	2.5097W	2.5566W	0.9817
$70W/m^2$	2.9815W	3.0391W	0.9810
$80W/m^2$	3.4600W	3.5293W	0.9804
$90W/m^2$	3.9459W	4.0261W	0.9801
$100W/m^2$	4.5274W	4.5289W	0.9997

#### 4 Flowchart of the proposed MPPT algorithm

The control procedure cited above is summarized in the flow chart shown in Fig.10. First,  $m$  is defined zero, and the open-circuit voltage  $V_{oc}$  and the short-circuit current  $I_{sc}$ , which were measured at solar panel temperature  $25^\circ C$  and high irradiation  $1KW/m^2$ . The changing coefficient  $K_i$  of  $I_{sc}$  and the changing coefficient  $K_v$  of  $V_{oc}$  were measured. Second, The diode factor  $n$  and the reverse saturation current  $I_o$  are supposed. Third, the output current  $I(nl)$  and the output voltage  $V(nl)$  and the temperature  $T$  were detected by using sensors at time  $n1$ . Next, based on the supposed  $n$  and  $I_o$ , the photocurrent  $I_{ph}(n1)$  and the irradiation  $S$  were calculated. Then, the expiatory program is applied in order to acquire the supposed maximum power  $P_{max}'$ . Draw a comparison between the value of  $m$  and 10. If the value of  $m$  is less than 10, the value of  $m$  adds one. The actual maximum power point is gained by using the PO method under same weather conditions. The actual values of  $n$  and  $I_o$  are gained, and the values are saved, and the average values is calculated. Or else, the actual values of  $n$  and  $I_o$  were applied to acquire the maximum power  $P_{max}$  at the time, and the PO method is stopped. The proposed MPPT algorithm is high efficiency to track the maximum output

power of solar cell, and large numbers of calculation is not essential.

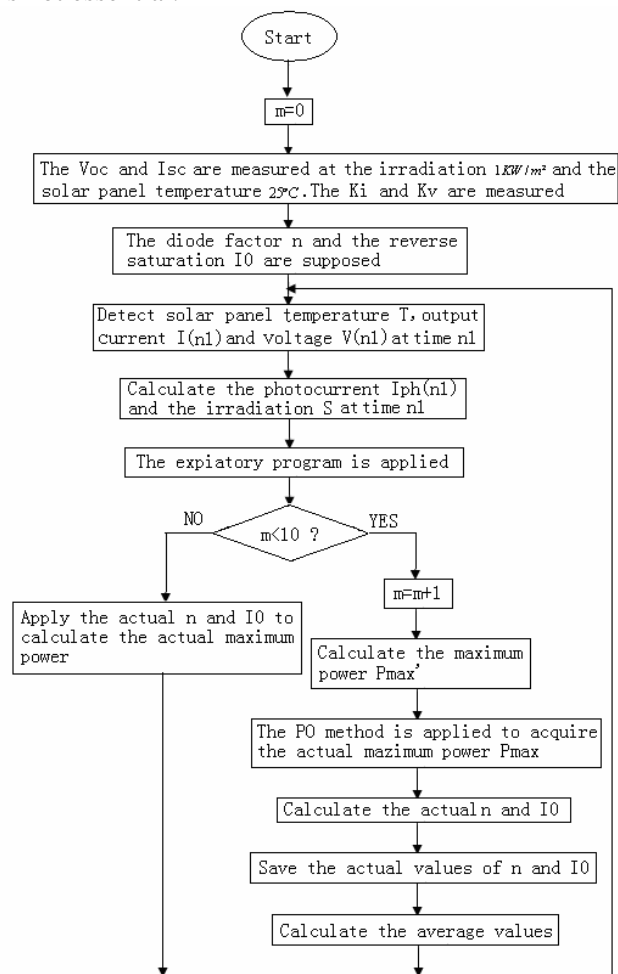


Fig.10 Flowchart of the proposed MPPT algorithm

## 5 Conclusion

In order to acquire the maximum power point of PV generate systems it is important to have an efficient MPPT algorithm. A novel MPPT algorithm was proposed in this paper. A new method of acquire the actual  $n$  and  $I_0$  are proposed by using the PO method. The expiatory program is applied to acquire the actual maximum power point. The correctness and validity of expiatory coefficients is verified through simulation under various weather conditions. The correctness and validity of expiatory coefficients is verified through simulation under different  $n$  and  $I_0$  conditions. In order to acquire the maximum power, the PO method is applied to acquire the actual  $n$  and  $I_0$ , but it is not applied to acquire the MPP in the whole tracking course, the loss of energy of solar cell is very small, and the output efficiency of proposed MPPT algorithm is more than 99%. In the future, the PI control of MPPT should be researched based on different load,

and the DC/DC circuit be used to track the maximum power point by controlling the switch frequency of IGBT. The intelligent theory should be used to improve PI characteristic, i.e., the fuzzy theory, the immune theory, and the nerve net theory etc.

## ACKNOWLEDGMENT

THIS PROJECT WAS GRANTED FINANCIAL SUPPORT FROM CHINESE POSTDOCTORAL RESEARCH FOUNDATION (NO: 2005038435), SHANGHAI BAI YU LAN SCIENCE AND TECHNOLOGY FOUNDATION (NO: 2007B073), AND CHINA EDUCATION MINISTRY RESEARCH FOUNDATION (NO: 20071108).

## References:

- [1] Yang Chen, Keyue Ma Smedley, A Cost-Effective Single-Stage Inverter With Maximum Power Point Tracking. IEEE Transactions on Power Electronics, Vol.19, NO.5, 2004, pp. 1289–1294.
- [2] K. K. Tse, Billy M. T. Ho, Henry Shu-Hung Chung, A Comparative Study of Maximum-Power-Point Trackers for Photovoltaic Panels Using Switching-Frequency Modulation Scheme, IEEE Transactions on Industrial Electronics, Vol.51, NO.2, April 2004, pp. 410-418.
- [3] Nobuyoshi Mutoh, Masahiro Ohno, Takayoshi Inoue, A Method for MPPT Control While Searching for Parameters Corresponding to Weather Conditions for PV Generate Systems, Industrial Electronics, IEEE Transactions, Vol. 53, NO.4, 2006, pp. 1055-1065.
- [4] Nobuyoshi Mutoh, Masahiro Ohno, Takayoshi Inoue, A Control Method to Charge Series-Connected Ultraelectric Double-Layer Capacitors Suitable for Photovoltaic Generate Systems Combining MPPT Control Method, IEEE Transactions on Industrial Electronics, Vol.54, NO.1, 2007, pp.374-383.
- [5] Peter Wolfs, Quan Li, A Current-Sensor-Free Incremental Conductance Single Cell MPPT for High Performance Vehicle Solar Arrays, Power Electronics Specialists Conference, 2006. PESC '06. 37th IEEE, 18-22 June 2006, pp.1–7.
- [6] W.J.A.Teulings, J.C.Marpinard, A.Capel, D.O' Sullivan, A new maximum power point tracking system, Power Electronics Specialists Conference, 1993. PESC '93 Record, 24th Annual IEEE, 20-24 June 1993, pp.833–838.

- [7] C. Hua and C. Shen, Comparative study of peak power tracking techniques for solar storage systems. Proc. IEEE Appl. Conf. and Expo, Vol. 2, Feb 1998, pp. 676–683.
- [8] Cristinel Dorofte, Uffe Borup, Frede Blaabjerg, A combined two-method MPPT control scheme for grid-connected photovoltaic systems. Power Electronics and Applications, European Conference, 11-14 Sept. 2005, pp.1-10.
- [9] M. Godoy Simoes, N. N. Franceschetti, M. Friedhofer, A fuzzy logic based photovoltaic peak power tracking controller, Industrial Electronics. Proceedings. ISIE '98. IEEE International Symposium on 7-10 July 1998, Vol.1, pp.300–305.
- [10] Tsai-Fu Wu, Chien-Hsuan Chang, Yu-Kai Chen, A fuzzy-logic-controlled single-stage converter for PV-powered lighting systems applications. IEEE Trans. Ind. Electron, Vol.47, NO. 2, Apr. 2000, pp. 287–296.
- [11] Majin, Reza Ahmadian, Gharaveisi, A.A., Khorasani, J., Ahmadi, M., Speed improvement of MPPT in photovoltaic systems by fuzzy controller and ANFIS reference model. WSEAS Transactions on Circuits and Systems, Vol.5, NO.8, August, 2006, pp. 1238-1243.
- [12] Ji, Changan, Zhang, Xiubin, Zeng, Guohui, He, Bin, Zhou, Xuelian, The study of the application based on fuzzy control for hybrid photovoltaic-wind renewable energy sources . WSEAS Transactions on Circuits and Systems, Vol.5, NO.1, January, 2006, pp. 9-16.
- [13] Theodoridis, Michael P, Axaopoulos, Petros, Architecture and performance of a power management system for multiple compressor solar ice-makers, WSEAS Transactions on Systems, Vol.6, NO.4, April, 2007, pp. 823-830.